Bijlage 1 – Geologische inventarisatie
Nederlandse samenvatting

GEOLOGISCHE INVENTARISATIE

CONCLUSIE
Een uitgebreide geologische studie is uitgevoerd door IF Technology. Als onderdeel van deze studie werden seismische gegevens geïnterpreteerd om de diepte van het reservoir, de Slochteren Formatie, af te leiden. Binnen het bestudeerde gebied wordt de diepte van de top van de Slochteren Formatie geschat op een diepte van circa 1.850 m. De dikte van de Slochteren Formatie wordt geschat op circa 60 m. Een petrofysische analyse werd uitgevoerd om de eigenschappen van het reservoir te analyseren. Uit deze analyse kan worden afgeleid dat de porositeit circa 22% is en de doorlaatbaarheid circa 500 mD. Deze reservoireigenschappen geven aan dat de Slochteren Formatie een goede potentie heeft voor aardwarmtewinning op de projectlocatie Luttelgeest.

Bijlage 1

GEOLOGISCHE INVENTARISATIE

INTRODUCTION

IF Technology executed extensive geological studies for the Luttelgeest project area as part of SDE+ and RNES subsidy applications. Seismic data was interpreted and a petrophysical analysis was performed. From these analyses the depth, thickness, porosity and permeability of the target reservoir for geothermal application, the Slochteren Formation, is determined. The sections below give a description of the work performed and present the results.

REGIONAL SETTING

The target unit for this study is the Slochteren Formation of the Upper Rotliegend Group. The regional and local geological setting is therefore described from the Late Carboniferous onwards.

The study area is dominated by the Texel IJsselmeer High, which is a NW-SE striking tilted fault block which has been a structural high since Carboniferous times (Rijkers and Geluk, 1996). During the Early Permian the Southern Permian Basin developed as a result of rifting and associated subsidence. This basin extended from England to Poland. Luttelgeest was situated close to the north flank of the Texel-IJsselmeer High that functioned as a barrier within the Southern Permian Basin.

During the Late Permian, this high influenced the deposition of the Zechstein Formation. On the flanks of the high, an extensive carbonate and anhydrite platform formed (Rijkers and Geluk, 1996 and references therein). At the end of the Permian, differential subsidence ceased. In the early Triassic a large floodplain developed and associated deposits were formed. After the uniform development of the basin during the Early Triassic, structural elements of the Permian were again accentuated later in the Triassic. The deposition of Triassic deposits focused on subsiding areas while in the region around Luttelgeest a thin succession of the Triassic sediments was deposited. Continuous basin subsidence and sea level rise resulted in a transgression. Younger Triassic sediments were likely deposited within the study area but have later been eroded. In the same erosion phase all Jurassic deposits have been eroded as well. The exact influence of the Kimmerian tectonic phase responsible for this erosion is difficult to assess as the hiatus extents over the complete sedimentological interval. During the Jurassic and Early Cretaceous the Friesland Platform and the Texel-IJsselmeer High, developed from the Netherlands Swell. A map of the structural elements formed during the Late Jurassic to Early Cretaceous is shown in Figure 1.

At the end of the Kimmerian tectonic phases, the tectonic regime switched to a regional subsidence. After a period of relative rest, the region was uplifted again as a result of the collision between Africa and Europe. At the end of the Cretaceous, several basins were inverted. This inversion resulted in truncation of the Maastrichtian sediments on the Texel-IJsselmeer High (Figure 2). After these tectonic phases the North Sea Basin developed which is still influencing sedimentation to date. Salt movement has been of little influence on sedimentation and erosion on the Friesland Platform (Ten Veen, van Gessel, and den Dulk, 2012).

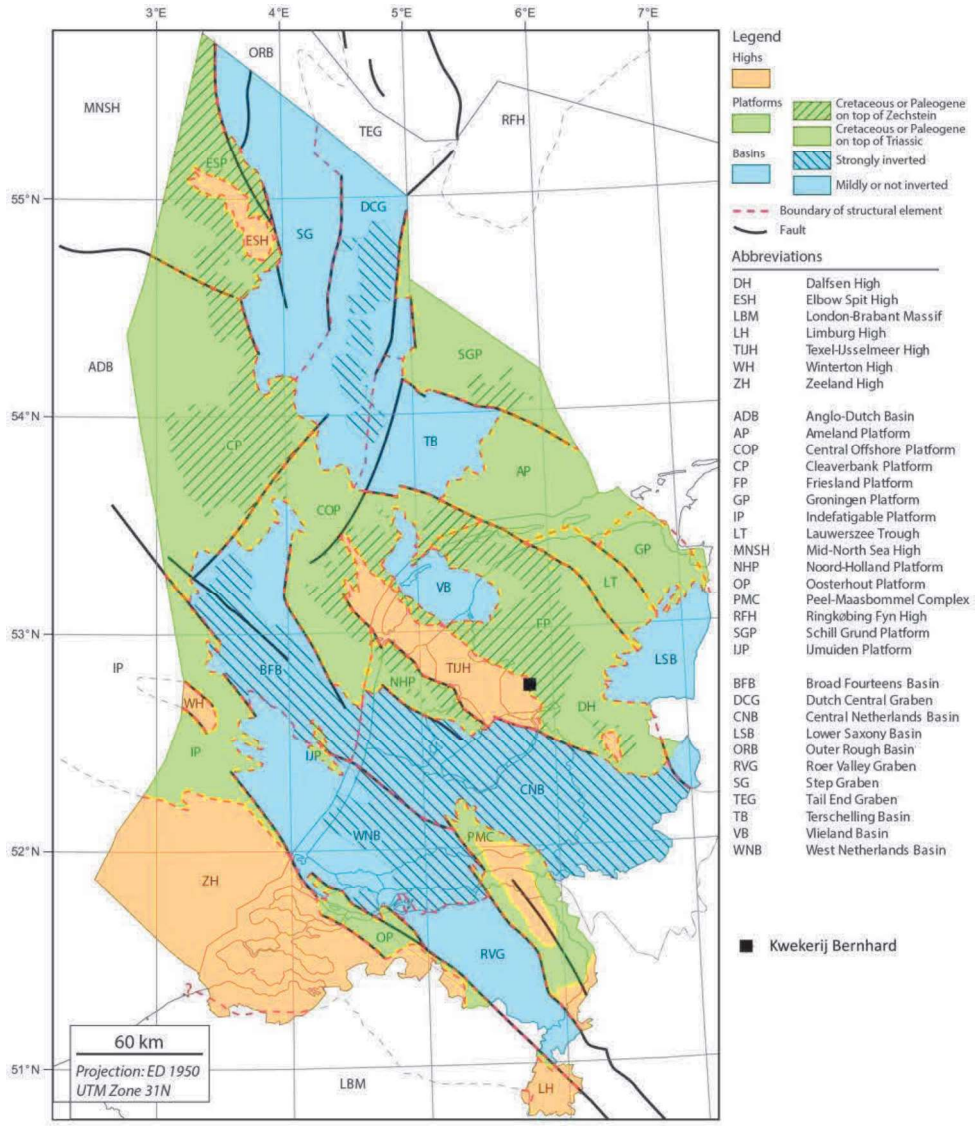

Figure 1. Location of the project with respect to the Jurassic/Cretaceous structural elements (after Kombrink et al., 2012).

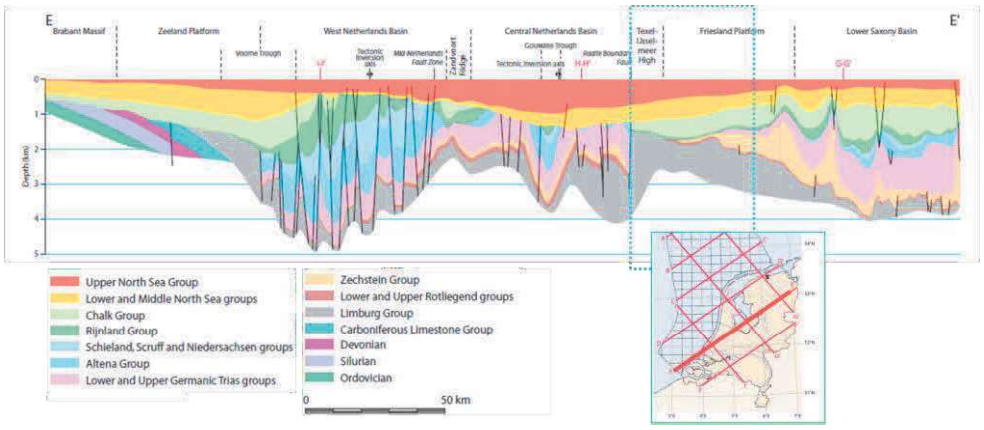

Figure 2. Schematic transect showing the regional geology and stratigraphy at the project area, highlighted by the blue dotted box.

LOCAL GEOLOGY

The subsurface of Luttelgeest consists of different layers and lithologies. Table 1 shows the proposed stratigraphy based on the interpretation of wells LTG-01, EMO-01 and the seismic data. Seismic data shows that the stratigraphy of LTG-01 and EMO-01 are the most representative for the area. It should be noted that the presence of Zechstein sediments is not certain. Seismic interpretation indicates a possible presence. If Zechstein is present, it is expected to consist of limestones and/or claystones.

	Top [mTVDSS]	Base [mTVDSS]
North Sea Supergroup	0	-1130
Chalk Group	-1130	-1660
Rijnland Group	-1660	-1845
Zechstein Group	-1845	-1850
Upper Rotliegend Group	-1850	-1910
Limburg Group	-1910	Not mapped

Table 1. Expected stratigraphy.

GEOTHERMAL PLAY

The Slochteren Formation is part of the Upper Rotliegend Group and acts as the geothermal aquifer for the proposed geothermal play. The Slochteren Formation consists of continental course grained sandstones, conglomerates and aeolian deposits. These were deposited in the Southern Permian Basin when a desert-like environment was present at the location of Luttelgeest. The sediment source of these deposits were the Variscan mountains, situated to the south and southeast of Luttelgeest. The course sandstones and the conglomerates are interpreted as alluvial fan deposits and proximal river deposits. The aeolian deposits have been transported by trade winds from a large area from the east (TNO-NITG 1993).

The seismic data shows that the Slochteren Formation is onlapping onto the Texel-IJsselmeer High. It is likely that the sedimentation rate near the high was slower which may have influenced the variation in thickness of the formation and explain the onlapping geometries. The thickness of the

Slochteren Formation has also been strongly influenced by the Kimmerian tectonic phases when the Slochteren Sandstone was eroded at the crest of the Texel-IJsselmeer High (Rijkers and Geluk, 1996). This explains the difference in thickness where Cretaceous deposits are found directly on top of the Slochteren Sandstone as is the case in the area around Luttelgeest.

Well logs in the project area report that the Slochteren Formation consists of reddish sandstones. The red colour is of early diagenetic origin when the environment was oxidizing with a high degree of acidy. Also, reports are made on friable and poorly cemented zones within the formation. The high porosity zone where Luttelgeest is situated is likely due to leaching during the Mid-Late Jurassic as a result of the Kimmerian uplift (TNO-NITG 1993). This clearly shows the influence of the uplift of the Texel-IJsselmeer High on the sedimentary and diagenetic processes within the Slochteren Formation.

The Slochteren Formation is proven to be present in the Luttelgeest project area with the successful drilling of three recent geothermal wells; LTG-GT-01, LTG-GT-02 and LTG-GT-03.

PRESENCE OF HYDROCARBONS

Figure 3 shows the hydrocarbon fields in the vicinity of the exploration license. The Marknesse field, drilled by the MKN-01 well in 1983, has its reservoir in the Dongen Tuffite Member of the Tertiary. Gas has also been encountered in the Zechstein Formation. The currently producing Wanneperveen field, discover in 1951, is located to the east of the Luttelgeest exploration license area. This field is producing from multiple reservoirs: the Basal Dongen Tuffite Member, the Vlieland Sandstone Formation and the Lower Buntsandstein Formation.

None of the gasfields are located in the Slochteren Formation. None of the surrounding wells have encountered gas accumulations in the Slochteren Formation. There is a small chance of encountering free gas at the Zechstein level.

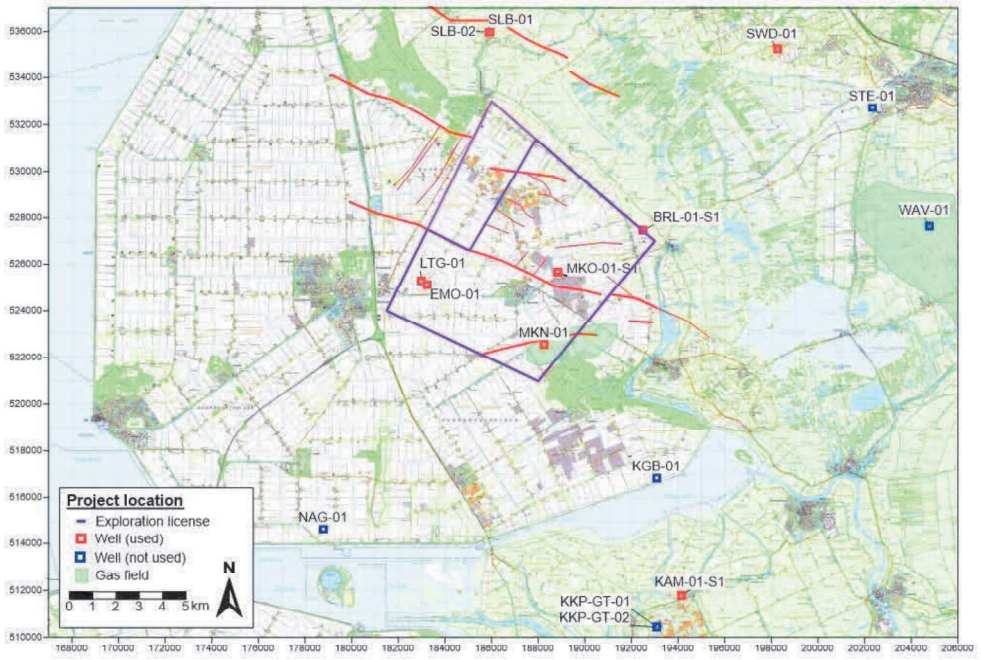

Figure 3. Location of the exploration license (purple/pink) with respect to hydrocarbon fields.

AVAILABLE AND USED DATA

Wells

Wells have been drilled in the surrounding area of Luttelgeest for the exploration of hydrocarbons. These wells all contain data that can be used to assess the Slochteren Formation for its depth, thickness and reservoir properties. Table 2 lists the wells in the immediate surroundings of the project location and for what purpose they have been used. These wells are plotted in Figure 4. Wells NAG-01 and KGB-01 were excluded from the petrophysical analysis because of limitations on the well logs available. Although well KAM-01-S1 is located relatively far from the project location it was included in the petrophysical analysis, because of the available core data.

Well	Spud year	used for Petrophysics	Used for seismic interpretation	Used for thickness-map / temperature gradient
BRL-01-S1	1981	X	X	X
EMO-01	1986	X		X
KAM-01-S1	1969	X		X
LTG-01	2004	X	X	X
MKN-01	1983	X	X	X
MKO-01-S1	1986	X	X	X
SLB-01	1983	X	X	X
SLB-02	1986	X	X	X
SWD-01	1966	X		X
NAG-01	1970			X
KGB-01	1987			X

Table 2. Overview of the wells used in the study.

Seismic data

The area around Luttelgeest is not covered by 3D seismic data and therefore 2D data was used. The area of interest is covered by lines with approximately 1-2 km line spacing. This dataset is available in the public domain and the lines have been selected based on their quality. The lines are shown in Figure 4.

All seismic images within this report are displayed according to the non-SEG display convention. This means a hard kick is displayed in red (or white) and a softkick is displayed in blue (or black).

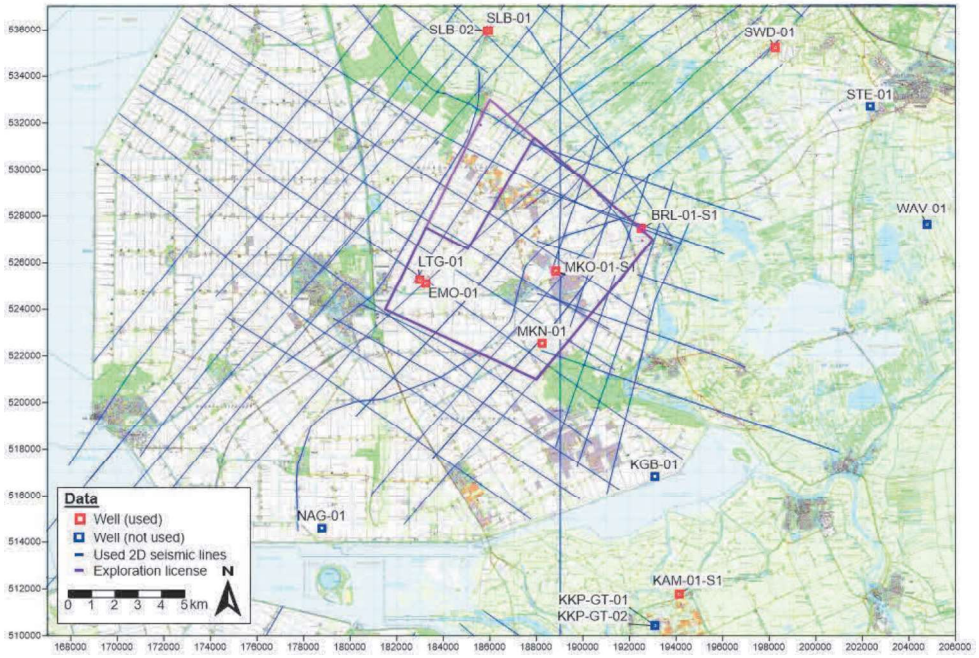

Figure 4. Data used.

Coordinate reference system

All data was delivered in the Rijksdriehoek (RD) coordinate system. Whenever the data was not yet available in this datum, it was converted into RD. Data in UTM31 was converted to RD using Surfer 13.6

SEISMIC INTERPRETATION AND DEPTH MODEL

Methods

The seismic data was interpreted using the software OpendTect. At the time of the interpretation, version 5.0.4 was available. There were no known bugs at the time that would have influenced the interpretation process or its results. SMT Kingdom was used to calculate the mis-ties between the 2D seismic lines. The important horizons and faults present within the Slochteren Formation were

interpreted. Subsequently the horizon interpretation was exported to a GIS program for gridding and visualizing the final maps.

Since it transpired that lines 865007 and 815019R were not positioned on their correct locations they were omitted from the dataset.

Additional data

The existing reports of Panterra in this area have been used as well as the information on Kaartblad V (Panterra 2013, 2012a, 2009; TNO-NITG 1993).

Well to seismic ties

Of the wells LTG-01, SLB-01, SLB-02, MKO-01-S1, MKN-01 and BRL-01-S1, synthetics were made. As an example, **Fout! Verwijzingsbron niet gevonden.** shows the synthetic of SLB-01 in line with part o f seismic transect 803005. All the other wells also tie to the seismic data.

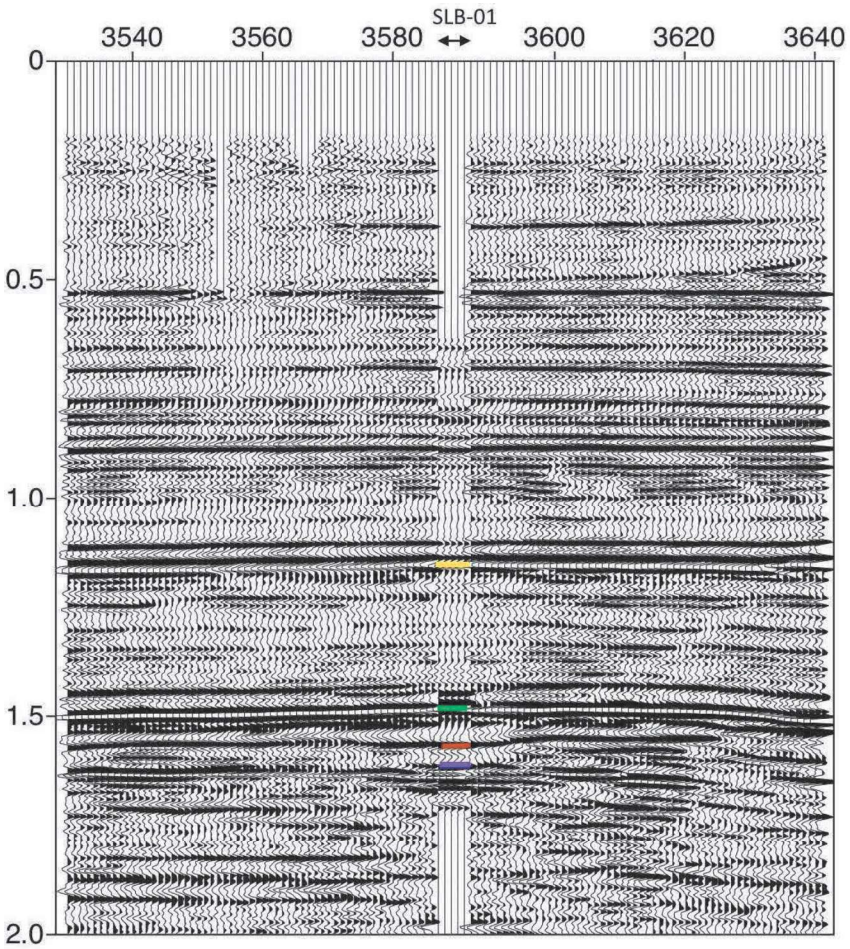

Figure 5. Synthetic of SLB-01 @ CDP 3586 of line 803005. Yellow: base North Sea Supergroup; green: base Cretaceous; brown: top Slochteren Formation; purple: Base Permian Unconformity.

Seismic interpretation

The mapped horizons were chosen based on their importance for the time-depth model. The selected horizons can easily be identified in the synthetics. The horizons that were interpreted and their characteristics are listed in Table 3. In Figure 6 and Figure 7 two seismic transects are displayed to illustrate the horizon and fault interpretation.

Horizon	Horizon code	Character	Quality
Base Tertiary Unconformity	BTU	Hard kick	Easy to interpret
Base Cretaceous Unconformity	BCU	Hard kick	Easy to interpret
Base Zechstein	BZE	Moderate soft kick	Not present everywhere, difficult to trace in places
Base Permian Unconformity	BPU	Hard kick, soft kick in places	In places difficult to trace across faults

Table 3. Mapped horizons and their characteristics.

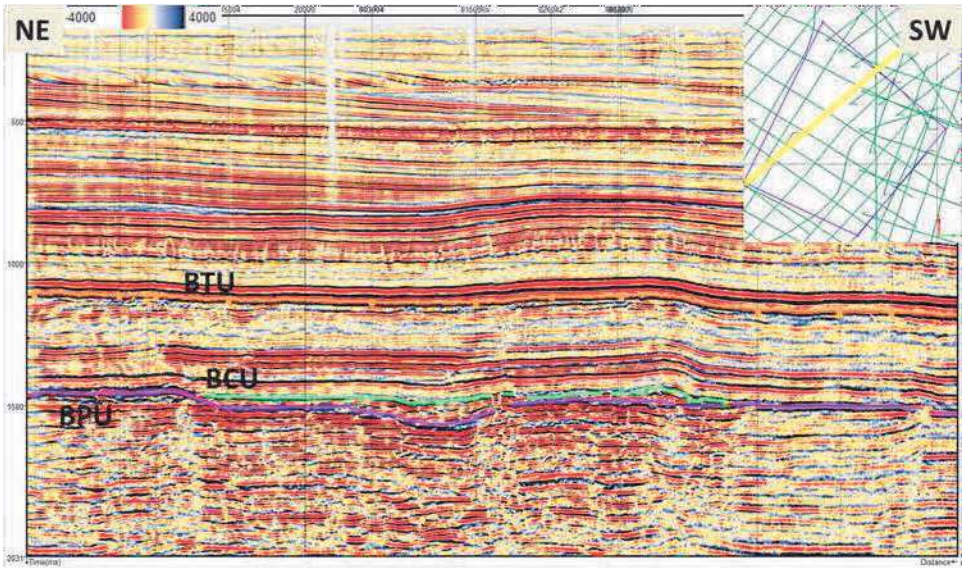

Figure 6. 2D seismic transect 803007 illustrating the interpretation of BTU, BCU and BPU.

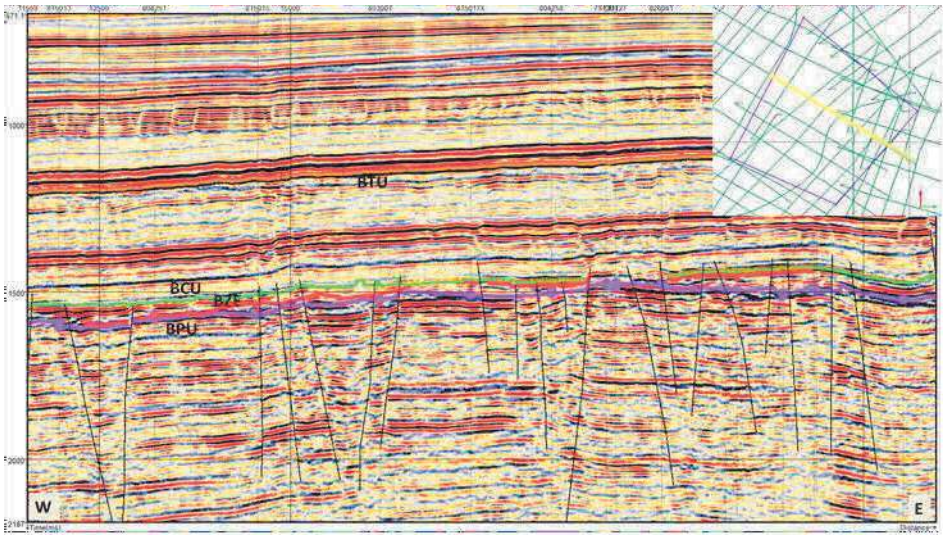

Figure 7. 2D transect 803004 showing the fault interpretation done by IF in 2015.

Temporal resolution

The temporal resolution at the level of the Slochteren Formation is approximately 11 ms. With an average interval velocity of 3800 m/s this corresponds to a resolution in depth of around 42m. The top and base of the Slochteren Formation (Base Zechstein and Base Permian Unconformity respectively) should therefore be individually visible on the seismic data in areas where the thickness is larger than 42 m. In areas where the thickness is smaller, the Δt is no longer representative for the Δz. The reflection disappears in areas thinner than 21 m (Kallweit and Wood, 1982).

Faults

In the subsurface of the area around Luttelgeest, faults can be clearly identified. Panterra identified the main fault direction as NW-SE to W-E in 2009 (Panterra, 2009). Panterra also reported that based on the information available from the gas exploration of the Slochteren Formation the faults are believed to be sealing. In the 2015 seismic interpretation study performed by IF Technology regional fault trends are interpreted. The line spacing between the 2D lines makes it difficult to confidentially trace the faults from one line to the next. Only a few bigger faults could be confidentially aligned.

The faults appear to be nearly vertical and steepen with depth. Most of the faults are ending at Base Permian Unconformity, only a few intersect both the Slochteren Formation and the overlying base Cretaceous sequence. Figure 7 shows a seismic transect illustrating the faults in the study area. In the area around the project location the faults occur in the lower part of the Slochteren Formation.

It should be kept in mind that the fault interpretation is based on 2D data only. This means that more faults might be present in between the lines which might act as barriers to flow. The offset at the level of the Slochteren Formation is limited, implying a sand-sand juxtaposition. The interpreted faults do not seem to extend over larger distances based on the current 2D interpretation. Therefore, small scale reservoir compartmentalization seems not quite probable. However, it cannot be excluded.

Gridding algorithm

Horizon grids are made based on the exported 2D seismic interpretation. The gridding method applied is based on inverse-distance squared weighting. Other methods were also tested, but did not result in significant differences.

Time-depth conversion

The time-depth conversion of this area is hampered by the relative thin layers. For the Tertiary interval as well as the Cretaceous interval it is no problem to establish a reliable interval velocity based on pseudo velocities. However, since the package from Base Cretaceous to Base Permian is on average less than 200 ms in time thickness, it is not possible to derive consistent and meaningful pseudo velocities. The velocities have also been calculated based on the synthetics in the available wells, but this also resulted in unrealistic large variations in interval velocities. Therefore, the choice has been made to define two intervals for the time-depth conversion. For the interval from the surface to the Base Tertiary Unconformity an uniform interval velocity of 1944 m/s is used. For the interval between Base Tertiary and the Base Permian Unconformity, a pseudo velocity grid based on the well velocities is used (Table 4). Figure 8 shows the applied interval velocities for the interval between Base Tertiary and Base Permian Unconformity. The higher values in SLB-01 and SLB-02 can be explained by the presence of anhydrite in the Zechstein interval.

Interval	Top horizon	Base horizon	Vint [m/s]
Tertiary	Surface/SRD	Base Tertiary Unconformity	1944
Cretaceous - Base Permian	Base Tertiary Unconformity	Base Permian Unconformity	**Fout! Verwijzingsbron niet gevonden.** - 2D variable

Table 4. Assumed interval velocities for the depth conversion method applied.

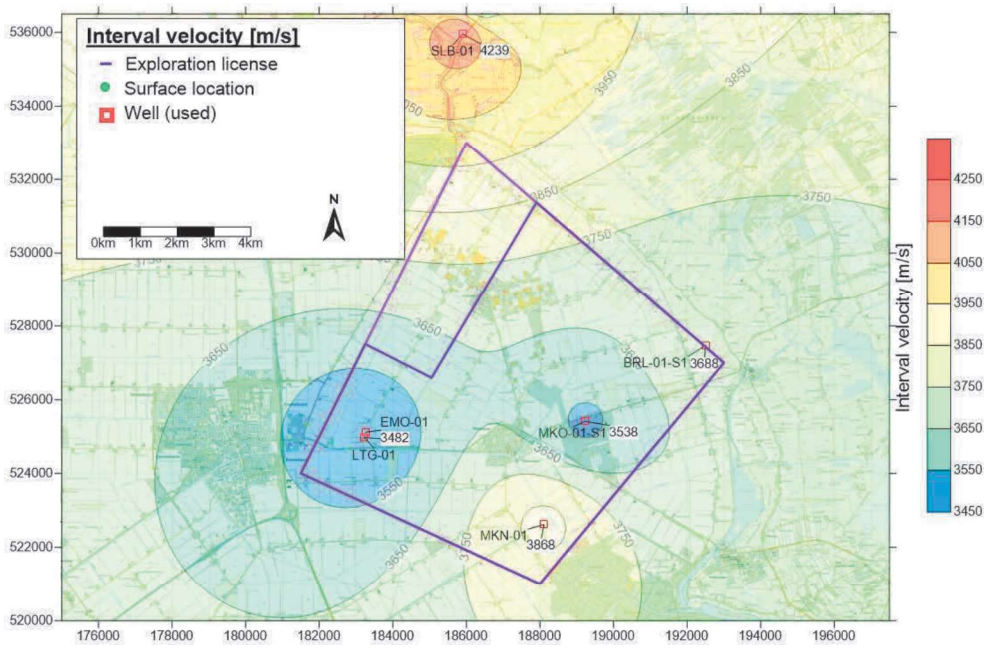

Figure 8. Interval velocities assumed between Base Tertiary and Base Permian. Luttelgeest geothermal exploration license areas in pink and purple.

Depth of top and base aquifer

The top of the aquifer could be identified on the seismic data. The Top Slochteren Formation corresponds with the Base Zechstein interpretation. The time grid has been converted to depth based on the time-depth conversion to result in the map displayed in Figure 9. The hatched areas indicate the locations where the Slochteren Formation is believed to be absent (Panterra 2012a). The base of the Slochteren Formation was interpreted as the Base Permian unconformity (Figure 10). It should however be noted that both horizons have been influenced by tuning due to the limited thickness.

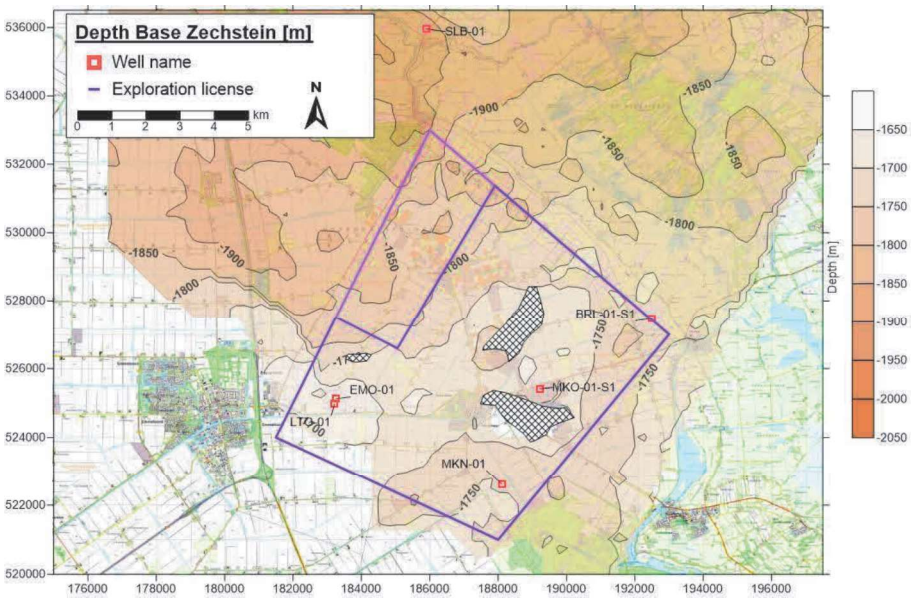

Figure 9. Depth of top Slochteren Formation, which is equal to depth Base Zechstein.

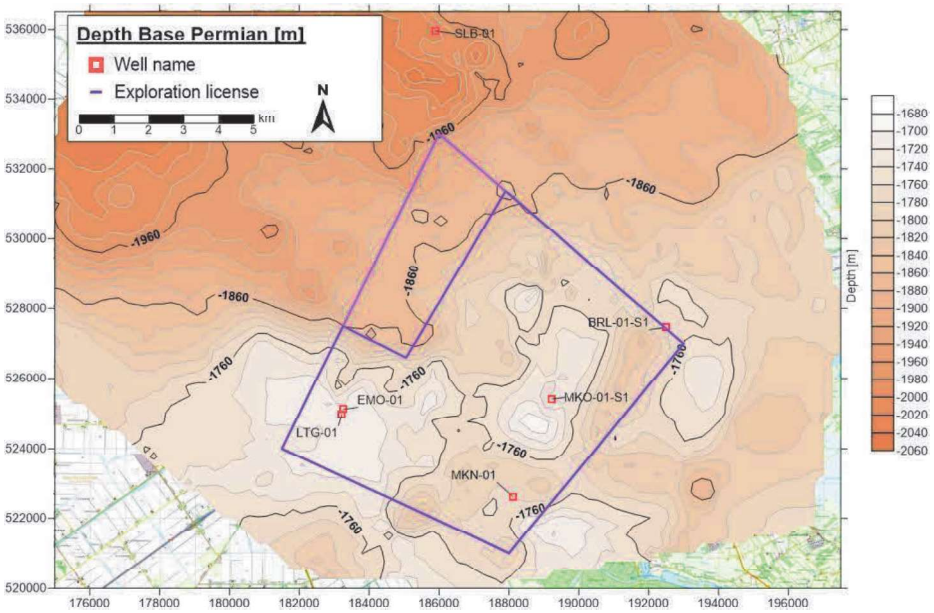

Figure 10. Depth of base Slochteren Formation, which is equal to depth Base Permian.

CHARACTERIZATION OF THE AQUIFER

Stratigraphical correlation and lateral variation

As discussed in the geological setting, the thickness of the Slochteren Formation around Luttelgeest is influenced by the presence of the Texel-IJsselmeer High in the south and southwest. This resulted in slower sedimentation rates and thus thinner deposits. The Kimmerian tectonic phases have also strongly influenced the thickness of the formation at and near the high where the deposits of the Cretaceous are unconformable overlying the Slochteren Sandstone. The seismic

interpretation results showed that the Slochteren Formation is absent in some places within the Luttelgeest exploration license (Figure 9). To the north and northwest, the Zechstein deposits appear in the lithostratigraphic column. This is shown in the correlation panel in Figure 11. The well locations are shown in Figure 4.

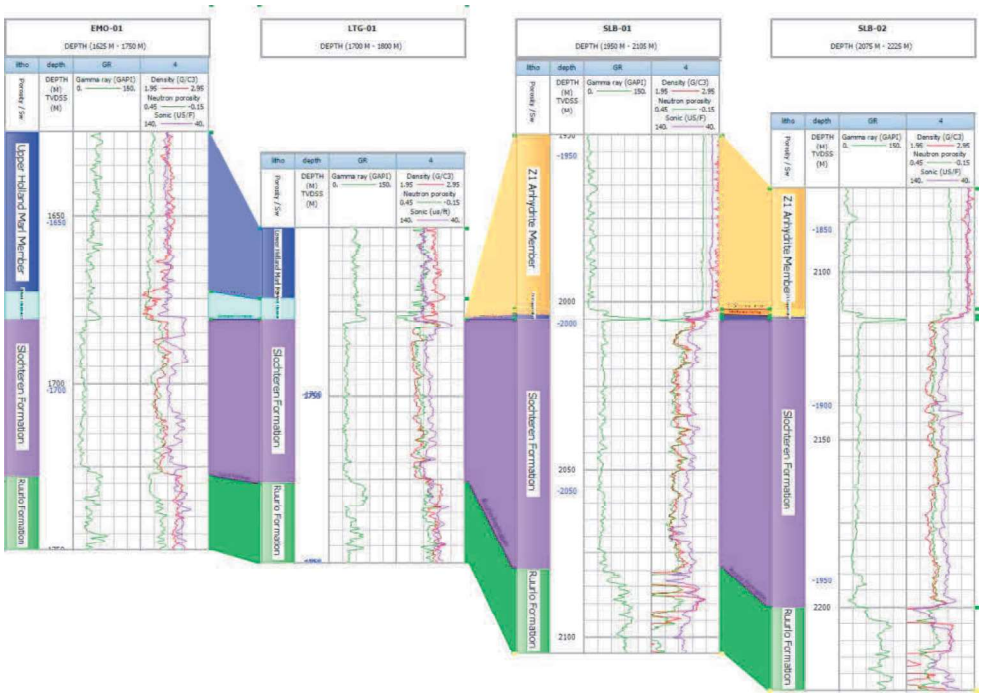

Figure 11. Correlation panel of EMO-01, LTG-01, SLB-01 and SLB-02.

Aquifer thickness

The thickness of the Slochteren Formation increases towards the north as shown in Figure 11. This corresponds with the regional pattern of the Slochteren Formation as reported by (TNO-NITG, 1993). The well BRL-01-S1 is an exception to this trend. The thickness of the Slochteren Formation is only 13 m at this location, which is significantly lower than the 92 m at MKO-01-S1 well. The thickness of the Slochteren formation is also significantly lower at the EMO-01 well. At this well a Base Zechstein unconformity is interpreted, which is a local disconformity not reported on the other wells in the area. The thickness variation from BRL01-S1 well to MKO-01-S1 well could explained by the fact that they are on different fault blocks.

Thickness of the reservoir formation can generally be approximated based on top and base of the reservoir when both are identified on the seismic data. However, since the thickness of the Slochteren Formation is within tuning distance within (parts) of the study area, the thickness determined from the seismic is not reliable. Based on the seismic data the Slochteren Formation is interpreted to be absent in certain places (see Figure 9, and Panterra 2012b). Therefore, it was decided to use the reservoir thickness map based on the well results for further calculations (Figure 12) combined with the seismic interpretation of the areas where Slochteren is believed to be absent (hatched areas on the map in Figure 9). This map was gridded using the inverse-distance weighting method.

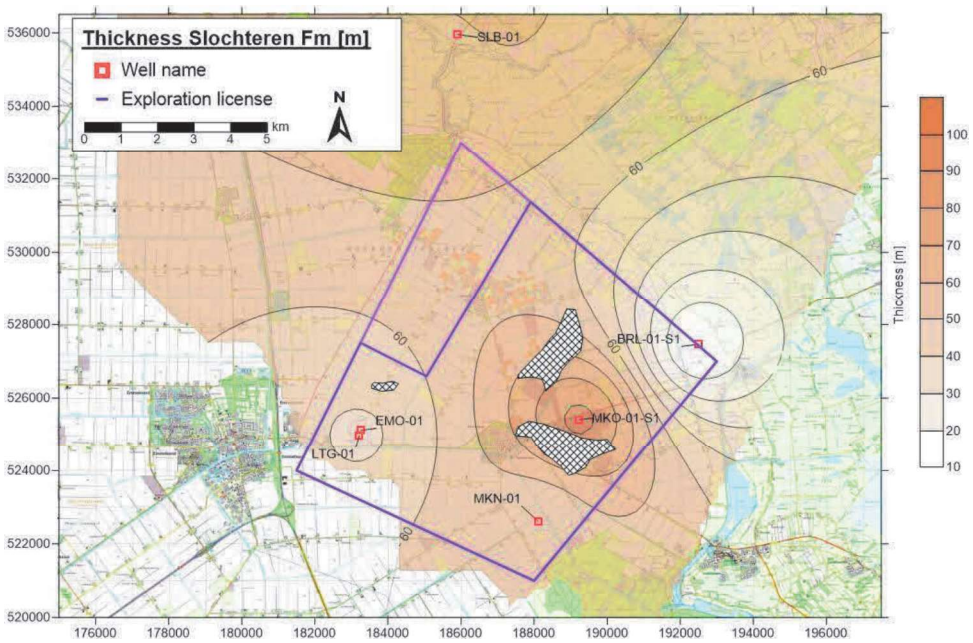

Figure 12. Gross reservoir thickness.

Petrophysical analysis

To determine the properties of the potential reservoirs, petrophysical analysis has been performed on 7 wells situated around the areas of particular interest around the license area. The surface locations of the wells are shown in Figure 4. An overview of the available logs measurements is given in Table 5.

Well	Spud year	Gamma Ray	Sonic	Density	Neutron porosity	Resistivity	Hydrocarbons Slochteren Fm.
BRL-01-S1	1981	X	X	X	X	X	
EMO-01	1968	X	X	X	X		
LTG-01	2004	X	X	X	X	X	
MKN-01	1983	X	X	X	X	X	X
MKO-01-S1	1986	X	X	X		X	
SLB-01	1983	X	X	X	X	X	X
SLB-02	1986	X	X	X	X	X	
KAM-01-S1	1969	X	X				
SWD-01	1966	X	X				

Table 5. Log measurements used.

Other wells more to the northeast have also reached the Slochteren Formation. However, these wells are located at greater distance and at the other side of a fault. For these reasons, these wells have not been considered. The other wells displayed in Figure 4 are not included since either the Slochteren Formation is not present there or has a gross thickness of less than 10m.

Sandstones do not solely consist of sand, but often also contain silt and clay fractions. The important properties which are determined in the petrophysical analysis include clay volume,

porosity, permeability and water quality. In this analysis, pore-filling is also determined. This may consist of water, oil, gas or salt. In the end, the permeability and net thickness of the reservoir determine the transmissivity.

Core measurements

Core measurements are present in some of the wells. The core measurements comprise porosity and permeability data. A short listing of the corrected core measurements for the Slochteren Formation can be found in Table 6.

Well	No. of measurements	Porosity [-]		Permeability [mD]	
		min	max	min	max
KAM-01-S1	54	0.095	0.200	0.1	15
MKN-01	38	0.180	00257	19	2481
SLB-01	40	0.040	0.233	3	824
SLB-02	27	0.146	0.245	74	1612
SWD-01	51	0.045	0.223	0.1	275

Table 6. Available corrected core data fort he Slochteren Formation.

Porosity

Porosity measurements have been carried out on the core samples under atmospheric pressure. To determine the porosity at depth, a correction factor needs to be applied. This factor is determined by the pressure within the reservoir. A correction factor of 0.95 has been applied. This factor is based on experience. The cores have also been shifted according to the porosity log.

Permeability

The measurements of permeability have been done under atmospheric pressure and using air instead of water. The air permeability differs from permeability for water. Furthermore, the permeability generally decreases with increasing pressure from overburden rock. Therefore, the data needs to be corrected. The measurements of the permeability have been corrected using the Juhasz compaction correction (Juhasz, 1986).

If $K_{air} > 660$ *mD*: (1)
$K_{brine}=K_{air}(PHIE/PHIT)^3$

If 160 *mD* $< K_{air} > 660$ *mD*: (2)
$K_{brine}=0.28K_{air}^{1.194}(PHIE/PHIT)^{3.045}$

If $K_{air} < 160$ *mD*: (3)
$K_{brine}=A\ K_{air}^{B}(PHIE/PHIT)^{C}$
With: $A = 4.14\ \sigma^{-0.390}$, $B = 0.80\ \sigma^{0.058}$ and $C = 2.04\ \sigma^{0.058}$

where K_{air} is the air-permeability, K_{brine} the water-permeability, PHIE the effective porosity fraction, PHIT the total porosity fraction and σ the isostatic stress in the reservoir in psi. The isostatic stress has been determined based on RFT measurements and assuming a Poisson's Ratio of

0.23. The overburden gradient has been determined using the general formula of 0.23*TVD. The calculated and applied isostatic stresses of each well are listed in Table 7.

Well	In situ stress [psi]
KAM-01-S1	1556
MKN-01	1429
SLB-01	1635
SLB-02	1551
SWD-01	1551*

*Table 7. Applied in-situ stress conditions. * no RFT was available. SLB-02 is in the same depth range and has a comparable lithostratigraphy as well as geological history and therefore the same stress has been applied.*

Porosity – permeability relationship

The porosity and permeability measured in the cores can be used to determine a direct relationship between the two. No distinction has been made between the Upper and Lower Slochteren Member. A further distinction based on facies was also out of the scope of this project. The data is shown in Figure 13.

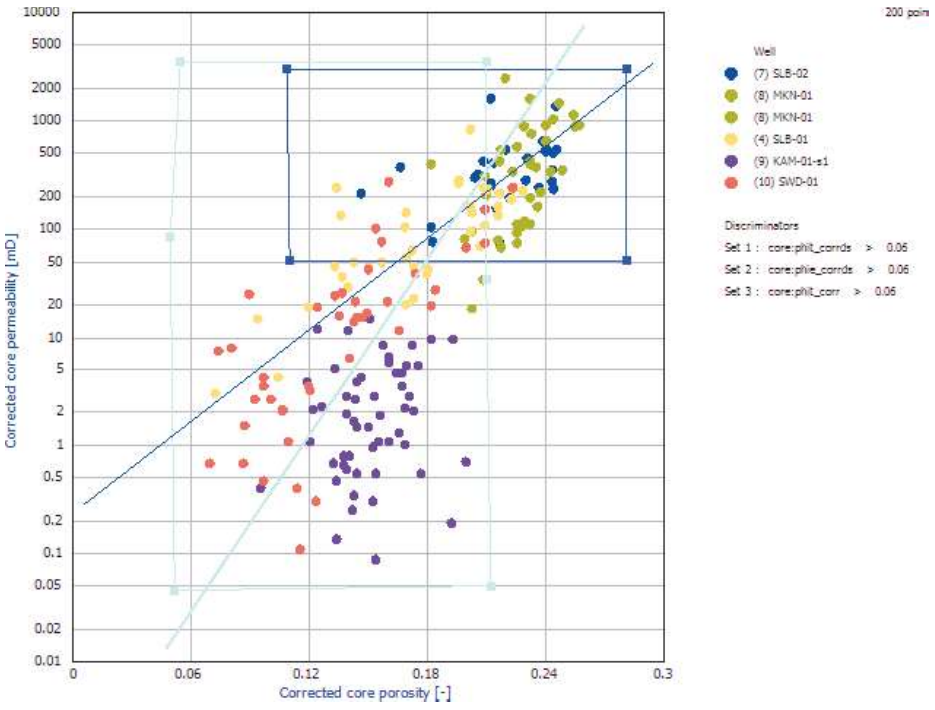

Figure 13. Porosity-permeability relationship of the Slochteren Formation.

The data allows for a porosity-permeability relationship which consists of two relationships and making the relationship more reliable at both the low end (in aqua) as well as the high end (in dark blue). Two areas have been defined:

- The first area includes all measurements with a porosity below 0.21,
- The second area includes all measurements with a permeability higher than 50 mD.

The relationship for each area has been determined using RMA regression. The porosity-range determines which relationship is valid, this range is defined by the intercept of the two regression lines. The relationships can be described as:

$$(1) \quad \emptyset < 0.195 \qquad Kh[mD] = 10^{-3.16348+27.1335\emptyset}$$
$$(2) \quad \emptyset > 0.195 \qquad Kh[mD] = 10^{-0.62559+14.1456\emptyset}$$

Log interpretations

Well measurements have been used to determine the clay volume and the porosity of the Slochteren Formation. Where available, the porosity was determined based on the neutron- and density logs. When the neutron log was missing, the density has been used. The sonic log has been used to separately calculate the porosity for the validation of the porosity determined from the neutron-density method. The important assumptions are listed in Table 8.

Saturation equation	[-]	Indonesian
PhiT Clay	[-]	0.1
a-factor	[-]	1
m-exponent	[-]	2
n-exponent	[-]	2
Clay volume cut-off	[-]	0.4
Porosity cut-off	[-]	0.06
Applied sonic equation	[-]	Raymer (sand 55, water 190)

Table 8. Assumptions and cut-offs used for all wells.

The resulting porosities have been compared to the porosity of the core measurements. Core shifts have been applied. Figure 14 gives the correlation between the calculated and the measured porosity for SLB-01/02 and MKN-01. Ideally, correlation between calculated and measured porosity is equal to one. All three wells show that the calculated porosity is 2% lower than the corrected core porosity.

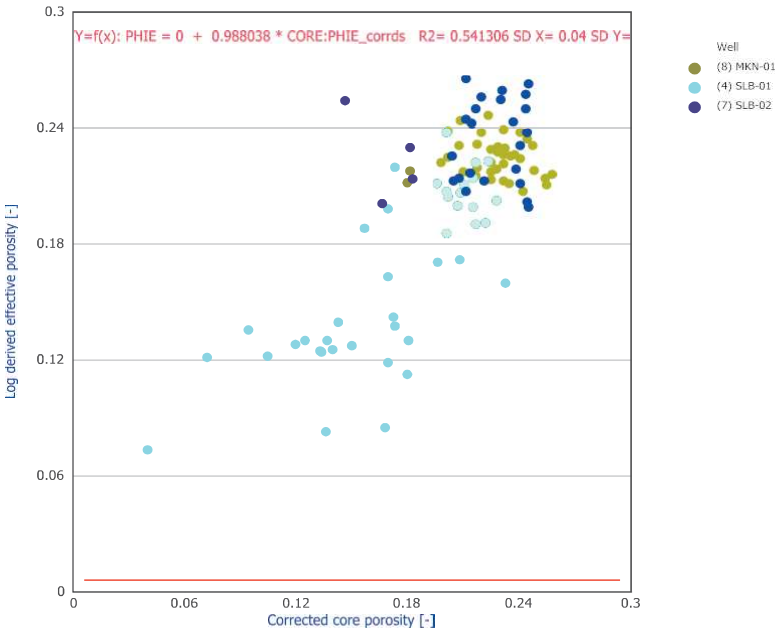

Figure 14. Examples of log-derived porosity versus corrected core porosity.

The porosity log has been used to calculate a permeability log based on the porosity-permeability relationship reported above. The transmissivity is determined by multiplying the mean permeability with the net reservoir thickness. The mean permeability can be determined using different methods, depending on the depositional environment. Here, the reservoir is considered to be a more or less laterally continuously layered medium to which an arithmetic average applies (Eschard et al., 1998). As such, the following relationship has been used:

$$\bar{k} = \frac{1}{n}\sum_{1}^{n} k^{\omega}_{i} \qquad (7)$$

Where k denotes permeability and ω is power exponent as defined by (Herweijer, 1997). In the case of the arithmetic mean, ω reverts to 1.

Monte Carlo analysis

For each well, a Monte Carlo analysis has been run within Interactive Petrophysics. In this module, the deterministic values are shifted by standard uncertainties of each curve. The module was run for 200 iterations and resulted in distribution of the important parameters. The parameters which were exported include the net thickness, Net/Gross, average effective porosity, and the average permeability.

The permeability of the reservoir has been calculated based on the porosity log and the here reported porosity-permeability relationships. The reservoir is considered to be a more or less laterally continuous layered medium to which an arithmetic average applies. For each well, the Monte Carlo uncertainty simulation within IP has been run, resulting in an uncertainty of the net thickness, N/G, average porosity and average permeability.

Table 9 shows the deterministic results of the log evaluation of each well.

Well	Top interval [m MD]	Base interval [m MD]	Top interval [m TVDSS]	Base interval [m TVDSS]	Gross thickness [m]	Net thickness [m]	N/G [-]	Average porosity [-]	Average permeability [mD]	Transmissivity [Dm]
BRL-01-S1	1760.5	1773.2	-1752.3	-1764.9	12.6	8.3	0.6539	0.0929	0.4	0.0
EMO-01	1680.8	1727.8	-1678.8	-1725.8	46.9	45.3	0.9644	0.2513	1136	51.4
LTG-01	1727.0	1776.0	-1677.6	-1726.5	48.8	47.9	0.9809	0.2574	1396	66.8
MKN-01	1686.9	1756.1	-1659.4	-1728.6	69.2	68.9	0.9959	0.2157	425	29.3
MKO-01-S1	1755.0	1857.0	-1675.5	-1767.1	91.6	89.3	0.9753	0.2549	1306	116.6
SLB-01	2005.0	2079.7	-1998.7	-2085.8	74.6	72.9	0.9767	0.1927	267	19.5
SLB-02	2114.0	2200.0	-1875.3	-1957.6	82.2	81.7	0.9934	0.2035	276	22.5

Table 9. Deterministic results of the log evaluation.

Extrapolation of porosity and permeability to the projects location

In previous studies the porosity and permeability were linearly interpolated between the wells. Alternatively, it was suggested to use a logarithmic approach for the permeability. The question is whether this is representative or applicable. In the previous studies a permeability-depth relationship has not been used or discussed.

Extrapolation can be done based on permeability-depth relation. However, this does not take into account the influence of the thickness of the Zechstein formation. The results show that the porosities are significantly higher within the area where the Zechstein deposits are absent or very thin. As a consequence, the question can be asked whether the permeability-depth relationship is applicable. Considering the limited number of wells in the area where the Zechstein is absent, a separate relationship cannot be sufficiently underpinned.

Another thing to keep in mind is the local presence of anhydrite cemented parts of the Slochteren Formation such as encountered in the KKP-GT-01/02 wells. None of the wells in the surrounding area show the same log response as encountered in KKP-GT-01/02. Since it is a local phenomena according to Henares et al. (2014), the chances are that cemented parts have been missed by the drilled wells and they are present in the region. However, the geological history differs from the area around Koekoekspolder which resulted in leaching of the Slochteren Formation in this area in contrast to that in Koekoekspolder (TNO-NITG, 1993)

The extrapolation has been done based on the porosity-depth relationship between the wells. This relationship is given by:

$$\emptyset_{average} = 1.716E^{-4}z + 0.533$$

Where Φaverage is the average porosity and z is the depth in negative TVD. The relationship is plotted in Figure 15. The resulting porosity map is shown in Figure 16.

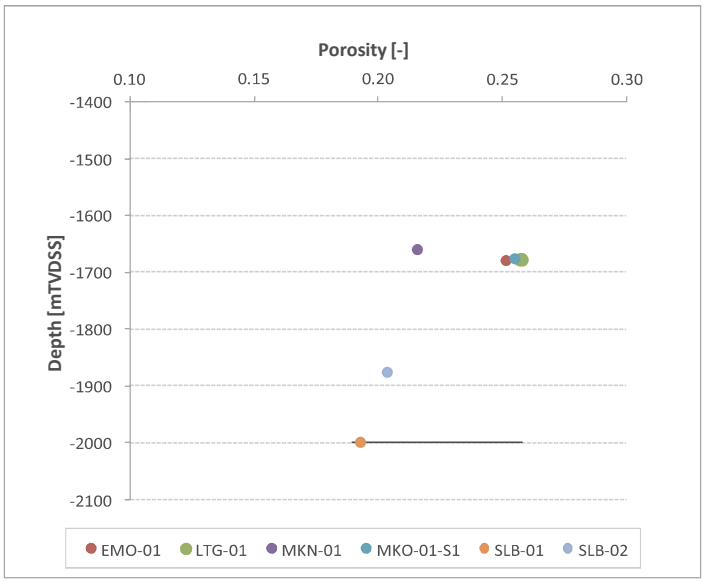

Figure 15. Average porosity-depth relationship.

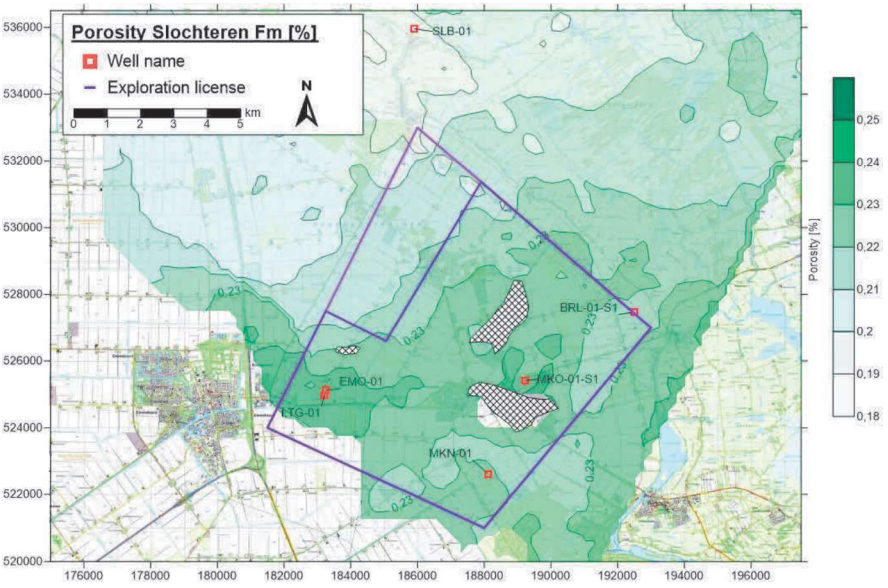

Figure 16. Average porosity map of the Slochteren Formation.

The permeability has then been determined based on the average porosity-average permeability relationship:

$$K_{average} = 1.2457e^{27.183\emptyset_{average}}$$

Where Kaverage and Φaverage are the average permeability and porosity respectively. The relationship is also plotted in Figure 17. The resulting permeability map is shown in Figure 18.

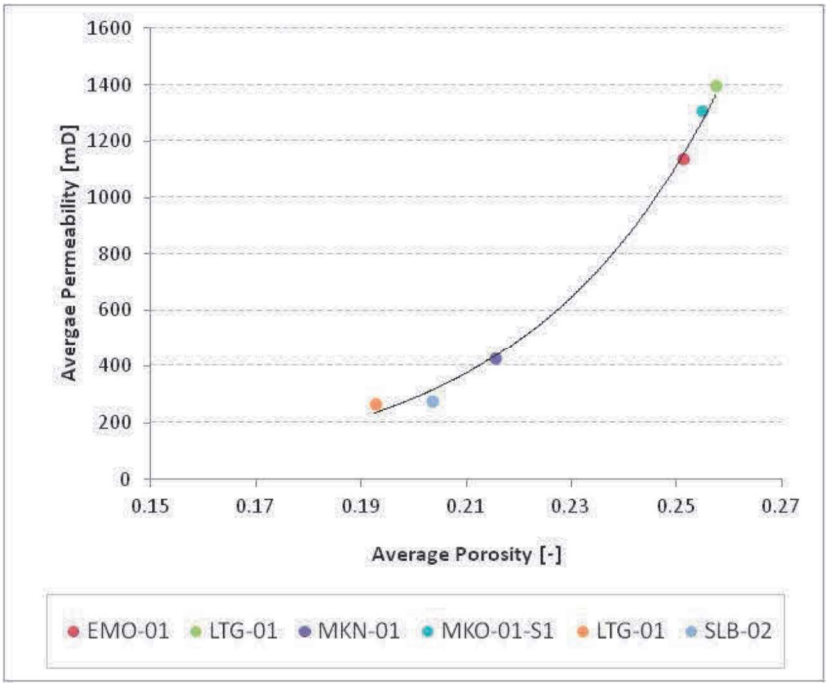

Figure 17. Average porosity vs average permeability.

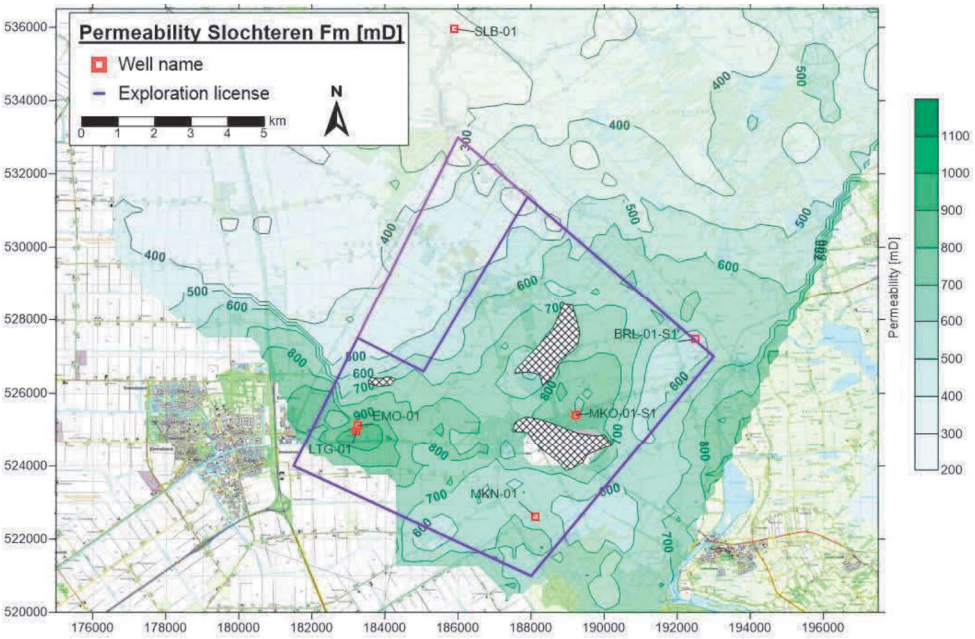

Figure 18. Average permeability map of the Slochteren Formation.

WATER EVALUATION

Temperature

IF Technology calculated the temperature gradient based on corrected Bottom Hole Temperatures (BHT's) reported by the wells in the study area. The reported BHT's in the different wells logs were corrected using the Horner method. Measurements with a depth over 3030 m were not taken into account since it is known that the temperature gradient is different at greater depths in the wells LTG-01 and NAG-01. Following this approach, the temperature between 740 and 3,000 m can be represented by:

$$T = 0.0332z + 5.42$$

Where T is the temperature in °C and z the depth in meters. Figure 19 shows the temperature plot where the dotted lines show the 95% confidence intervals.

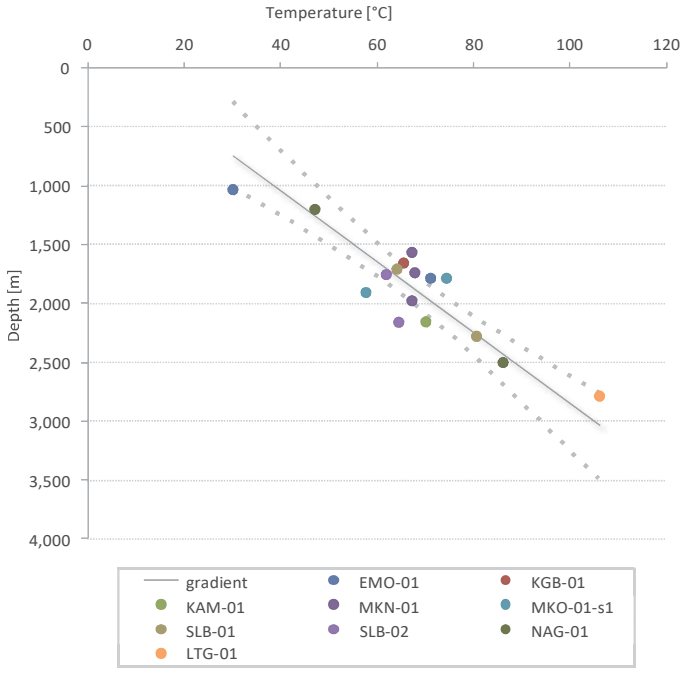

Figure 19. Temperature gradient for Luttelgeest and surroundings.

Following correspondence with TNO in June 2016 (Evaluation of SDE1637390) it was decided that the temperature gradient in the study area should be represented by the following formula:

$$T = 0.034z + 10$$

This formula is based on the temperature data of the wells in the vicinity of the project location and also takes into account the production water temperature at the geothermal project of Koekoekspolder (74 °C).

Evaluation of the formation water

Measured salinity

Only the composite well log of EMO-01 reports measured TDS values. During an open hole test as well as a FIT 210 g/l was measured. Assuming a density of the water of 1.11 g/l, this results in a salinity of approximately 190.000 ppm.

Log derived salinity

During the petrophysical analysis, the salinity of the water could be determined based on the porosity log and the resistivity logs. The resulting values are listed in Table 10. The results show an unrealistic low value for BRL-01-S1. This well will not be taken into account when determining the uncertainty. There is no explanation why this value is so low. The other values are slightly higher than the measured value in EMO-01. The highest values of SLB-01 and SLB-02 can be explained by the presence of thicker Zechstein salt deposits. Furthermore, they are located further away from the Texel-IJsselmeer High and thus the amount of leaching will have decreased.

Well	Rw	TDS [ppm]
BRL-01-S1		15.000
LTG-01	0.017	205.000
MKN-01	0.022	221.000
MKO-01-S1	0.020	218.000
SLB-01	0.020	235.000
SLB-02	0.020	245.000
EMO-01	0.023	190.000(1)

Table 10. Log derived salinity of the Slochteren Formation in ppm. (1) from FIT and open hole test

Hydrocarbons

Dissolved gas has been encountered in other nearby geothermal projects, Therefore the presence of dissolved gas cannot be excluded in this region. The maximum amount of dissolved gas can be approximated given the predicted water properties. For this location, the maximum amount of dissolved gas is 1.25 Nm^3/m^3 of geothermal brine. The likely occurrence of dissolved gas should be taken into account for the design of the system.

Aquifer pressure

Figure 20 shows the measured formation pressures through RFT's and the hydrostatic pressure gradient. The gradient has been calculated based on $P_{hydrostatic} = \rho * g * \frac{z}{100} + P_{surface}$, where ρ is the water density in kg/l, g the gravitational constant, z the depth in m, $P_{surface}$ the pressure at the surface. A water density of 1.15 kg/l, corresponding to the TDS value of 190,000 ppm and an injection temperature of 20 °C. The plot shows that the formation is under hydrostatic pressure.

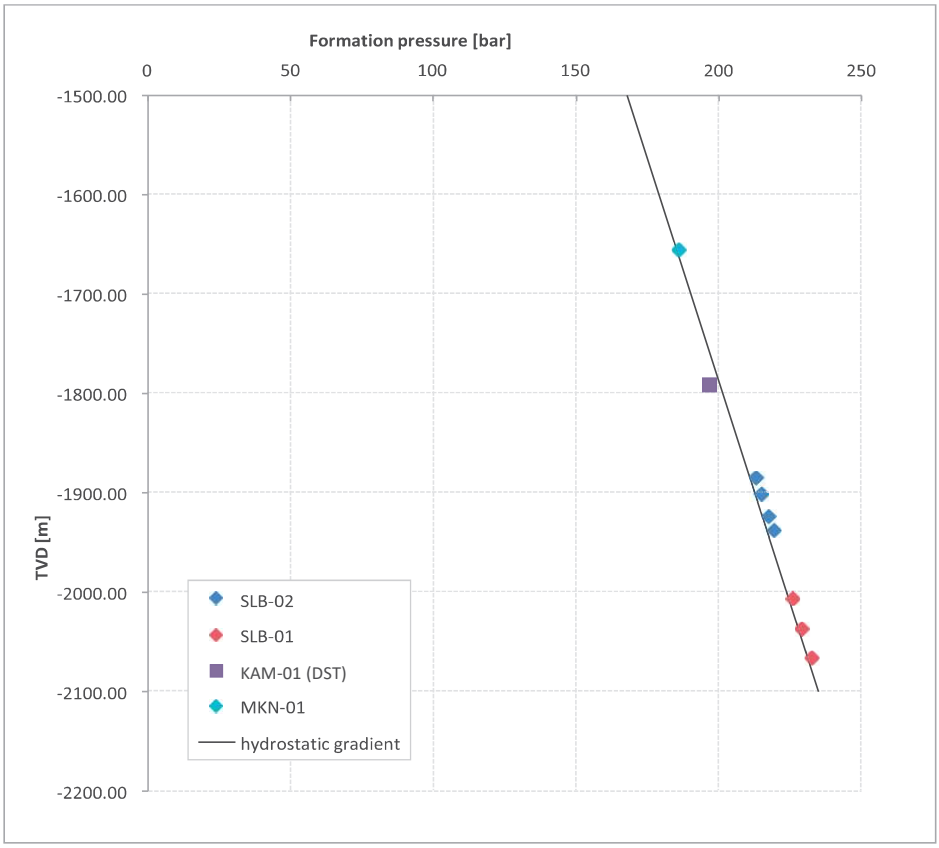

Figure 20. Measured formation pressures.

CONCLUSION

An extensive geological study was performed by IF Technology. As part of this study seismic data was interpreted to derive the depth of the target reservoir, the Slochteren Formation. The depth of the top of the Slochteren Formation is estimated to be at a depth of approximately 1.850 m within the study area. The thickness of the Slochteren Formation is estimated to be approximately 60 m within the study area. A petrophysical analysis was performed to analyse the reservoir properties. From this analysis it can be derived that the porosity within the study area is approximately 22% and the permeability is approximately 500 mD. These reservoir properties indicate that the Slochteren Formation has good potential for geothermal heat extraction at the Luttelgeest project location.

NL SUMMARY

CONCLUSIE

Een uitgebreide geologische studie is uitgevoerd door IF Technology. Als onderdeel van deze studie werden seismische gegevens geïnterpreteerd om de diepte van het reservoir, de Slochteren Formatie, af te leiden. Binnen het bestudeerde gebied wordt de diepte van de top van de Slochteren Formatie geschat op een diepte van circa 1.850 m. De dikte van de Slochteren Formatie wordt geschat op circa 60 m. Een petrofysische analyse werd uitgevoerd om de eigenschappen van het reservoir te analyseren. Uit deze analyse kan worden afgeleid dat de porositeit circa 22% is en de doorlaatbaarheid circa 500 mD. Deze reservoireigenschappen geven aan dat de Slochteren Formatie een goede potentie heeft voor aardwarmtewinning op de projectlocatie Luttelgeest.

REFRENCES

Duin, E.J.T., J.C. Doornenbal, R.H.B. Rijkers, J.W. Verbeek, and T.E. Wong. 2006. “Subsurface Structure of the Netherlands - Results of Recent Onshore and Offshore Mapping.” *Netherlands Journal of Geosciences* 85 (4): 245–76.

Eschard, R, P. Lemouzy, C. Bacchiana, G. Desaubliaux, J. Parpant, and B. Smart. 1998. “Combining Sequence Stratigraphy, Geostatistical Simulations and Production Data for Modelling a Fluvial Reservoir in the Chaunow Field (Triassic, France).” *AA* 82 (4): 545–68.

Henares, S., M. R. Bloemsma, M. E. Donselaar, H. F. Mijnlieff, A. E. Redjosentono, H. G. Veldkamp, and G. J. Weltje. 2014. “The Role of Detrital Anhydrite in Diagenesis of Aeolian Sandstones (Upper Rotliegend, The Netherlands): Implications for Reservoir-Quality Prediction.” *Sedimentary Geology* 314 (0): 60–74. doi:http://dx.doi.org/10.1016/j.sedgeo.2014.10.001.

Herweijer, J.C. 1997. “Sedimentary Heterogeneity and Flow towards a Well.” Amsterdam: VU.

IF. 2012a. “Addendum Op Puttest Injectieput Koekoekspolder KKP-GT-02.” Arnhem: IF Technology. P:\58351\SR\rapporten.

———. 2012b. “Addendum Op Puttest Productieput Koekoekspolder KKP-GT-01.” Arnhem: IF Technology. P:58351SRrapporten.

IF Technology. 2015. “Optimalisation Aardwarmte Luttelgeest.”

———. 2017. “SDE+ Application Hoogweg Paprikakwekerijen.”

Kallweit, R. S., and L. C. Wood. 1982. “The Limits of Resolution of Zero-Phase Wavelets.” *Geophysics* 47 (7): 1035–46. doi:10.1190/1.1441367.

Panterra. 2009. “Aardwarmte in de Noordoostpolder.” G743. Leiderdorp: Panterra. P:63341W02 eerdere rapportages Panterra.

———. 2012a. “Masterplan Aardwarmte Luttelgeest En Ens - Aanvullend Geologisch Rapport.” G950. Leiderdorp: Panterra. P:63341W02 eerdere rapportages Panterra.

———. 2012b. “Masterplan Aardwarmte Luttelgeest En Ens, Aanvullend Geologisch Rapport, G950.”

———. 2013. “Doublet Calculator Berekeningen Doublet 4, Luttelgeest.” Addendum G950. Leiderdorp: Panterra. P:63341W02 eerdere rapportages Panterra.

Rijkers, R.H.B., and M.C. Geluk. 1996. “Sedimentary and Structural History of the Texel- IJsselmeer High, the Netherlands.” In *Geology of Gas and Oil under the Netherlands*, by H.E. Rondeel, D.A.J. Batjes, and W.H. Nieuwenhuijs, 265–84. Kluwer Academic Publishers.

Ten Veen, J.H., S.F. van Gessel, and M. den Dulk. 2012. “Thin- and Thick-Skinned Salt Tectonics in the Netherlands; a Quantitative Approach.” *Netherlands Journal of Geosciences* 91 (4): 447–64.

TNO-NITG. 1993. “Toelichting Bij Kaartblad V Sneek-Zwolle.” In *Geologische Atlas van de Diepe Ondergrond van Nederland*, 126.